Biosensors and Bioelectronics 30 (2011) 151–157

Contents lists available at SciVerse ScienceDirect

Biosensors and Bioelectronics

journal homepage: www.elsevier.com/locate/bios

# Electrochemical synthesis of gold nanostructure modified electrode and its development in electrochemical DNA biosensor

Li Wang, Xiaohong Chen, Xiaoli Wang, Xiaoping Han, Shufeng Liu*, Changzhi Zhao*

*College of Chemistry and Molecular Engineering, Qingdao University of Science and Technology, Qingdao, Shandong 266042, China*

ARTICLE INFO

*Article history:*
Received 27 May 2011
Received in revised form 26 August 2011
Accepted 9 September 2011
Available online 16 September 2011

*Keywords:*
DNA immobilization
DNA hybridization
Gold nanostructure
Electrodeposition
Electrochemical biosensor

ABSTRACT

In this article, gold nanostructure modified electrodes were achieved by a simple one-step electrodeposition method. The morphologies of modified electrodes could be easily controlled by changing the pH of $HAuCl_4$ solution. The novel nanoflower-like particles with the nanoplates as the building blocks could be interestingly obtained at pH 5.0. The gold nanoflower modified electrodes were then used for the fabrication of electrochemical DNA biosensor. The DNA biosensor fabrication process was characterized by cyclic voltammetry and electrochemical impedance spectroscopy with the use of ferricyanide as an electrochemical redox indicator. The DNA immobilization and hybridization on gold nanoflower modified electrode was studied with the use of $[Ru(NH_3)_6]^{3+}$ as a hybridization indicator. The electrochemical DNA biosensor shows a good selectivity and sensitivity toward the detection of target DNA. A detection limit of 1 pM toward target DNA could be obtained.



## 1. Introduction

During the past decade, DNA biosensor has received substantial development in gene analysis, detection of genetic disorders, tissue matching, forensic and medical applications (Taton et al., 2000; Gunnarsson et al., 2008). Different techniques have been developed for DNA detection including fluorescence (Yang et al., 2008; Duan et al., 2007; Qiu et al., 2011), electrochemistry (Drummond et al., 2003; Liu et al., 2008; Zhang et al., 2009; Li et al., 2010), electrochemiluminescence (Zhu et al., 2008; Zhang et al., 2008b), chemiluminescence (Weizmann et al., 2003; Li et al., 2007), surface plasmon resonance spectroscopy (Kim et al., 2007; Seefeld et al., 2011) and quartz crystal microbalance (Patolsky et al., 2000; Minunni et al., 2005), etc. Among them, electrochemical technique affords a lot of advantages such as its simplicity, rapid, low-cost and high sensitivity (Munde et al., 2007; Sassolas et al., 2008). Currently, much effort has been devoted to upgrade the detection sensitivity and selectivity of electrochemical DNA biosensor (Kannan et al., 2011).

Recent developments in nanomaterials create many opportunities to advance DNA sensing and gene detection. The nanomaterials have been widely used as a medium of signal amplification to enhance the limit of DNA detection (Wang, 2003; Katz et al., 2004). For example, Chang et al. (2007) constructed a polyaniline nanotube array and realized an ultrasensitive detection of nucleic acid with a detection limit of 1.0 fM. Hu et al. (2008) developed a nanoporous gold electrode and achieved a detection limit of about 28 aM toward target DNA with the use of multifunctional encoded Au nanoparticle as signal amplification medium. Chen et al. (2009) developed a label-free dual sensing strategy toward DNA molecules using GaN nanowires and revealed excellent selectivity and specificity at picomolar concentration of target DNA. Soleymani et al. (2009) fabricated controlled Pd nanostructure modified electrodes and achieved the sensitive detection of DNA with the estimated detection limit of about 1 fM. Even though there are a lot of research works reported for electrode modification by different nanomaterials to improve the DNA biosensor performance, the preparation of nanomaterials or the electrode modification strategy is often relatively complex. Sometimes, the introduction of some organic molecules for example surfactant or polymer matrix in the preparation or assembly of nanomaterials often causes some uncertain effects in DNA detection. Furthermore, some DNA biosensors based on nanomaterial modification are still very limited for the improvement of DNA biosensor performance. Thus, the construction of nanostructure modified electrode by a simple strategy to improve the DNA detection sensitivity is highly desirable.

Among all kinds of nanomaterials, gold-based nanomaterials were the mostly used ones for the fabrication of electrochemical biosensor owing to its easy and rich surface function strategies and good biocompatibility (Liu et al., 2010). The gold nanomaterials could be easily attached on the electrode surface by some different strategies including direct electrostatic assembly, covalent linking, polymer entrapment or co-mixing, and electrodeposition methods.

* Corresponding authors. Tel.: +86 532 84022681; fax: +86 532 84022681.
*E-mail addresses:* sliu@qust.edu.cn, shufengliu77@yahoo.com (S. Liu), czzhao@qust.edu.cn (C. Zhao).

0956-5663/$ – see front matter © 2011 Elsevier B.V. All rights reserved.
doi:10.1016/j.bios.2011.09.003

The electrodeposition method is the most widely used approach for the substrate modification (Seo et al., 2011; Zhu et al., 2011). Gold nanostructures with different morphologies have been easily obtained by electrodeposition. For example, Guo et al. (2007a) prepared hierarchical flowerlike gold microstructures with gold nanoplates or nanopricks as building blocks by electrochemical deposition in a high concentration of 24.3 mM $HAuCl_4$ without introducing any template or surfactant. Zhang et al. (2008a) fabricated various gold nanostructures on glassy carbon electrodes in a low concentration of 5 mM $HAuCl_4$ solution by a simple one-step electrodeposition method. Li et al. (2011) obtained dendritic gold nanostructure modified electrode by electrodeposition in 2.8 mM $HAuCl_4$ and 0.1 M $H_2SO_4$ solution under a very negative potential of −1.5 V. Although electrodeposition has been demonstrated as an effective strategy for gold nanostructure modification, the role of nanostructuring in modulating biorecognition performance has been less addressed and needs further explored in detail, especially for these nanostructures with special morphology. The development of hierarchical nanostructures with novel morphology may provide a valuable platform for the applications in DNA biosensor, and even the protein, enzyme biosensor.

In this context, the hierarchical gold nanostructure modified electrodes were obtained by a simple electrochemical deposition method in a low concentration of 5 mM $HAuCl_4$ solution. The morphology of the final gold nanostructures could be easily controlled by simply changing the solution pH of gold precursors. Interestingly, a novel flower-like gold nanostructure with the nanoplates as the building blocks was obtained at pH 5.0. This gold nanoflower modified electrode has been demonstrated with an excellent capability for DNA immobilization and hybridization. With the use of $[Ru(NH_3)_6]^{3+}$ as an electroactive complex (Steel et al., 1998), the fabricated electrochemical DNA biosensor shows a very good selectivity and sensitivity toward the detection of target DNA. A detection limit of 1 pM toward target DNA could be achieved. The current electrode modification strategy is also expected to extend for the applications in protein, enzyme biosensor.

## 2. Experimental

### 2.1. Materials and chemicals

All of synthetic oligonucleotides were purchased from SBS Genetech. Co. Ltd. (Beijing, China). Their base sequences are as follows:

thiolated probe DNA sequence: 5′-SH-GCGCGAACCGTATA-3′;
complementary target DNA sequence: 5′-TATACGGTTCGCGC-3′; and
noncomplementary target DNA: 5′-ACTGATGCTACCAT-3′.

Hexaammineruthenium(III) chloride (RuHex) and 6-mercapto-1-hexanol (MCH) were purchased from Sigma (St. Louis, MO, USA), and tetrachloroaurate(III) tetrahydrate ($HAuCl_4{\cdot}4H_2O$, 47.8% Au) was obtained from National Chemical Reagent Ltd. (Shanghai, China). All other chemicals were all of analytical grade and used without further purification. Double distilled water was used throughout.

### 2.2. Apparatus

Cyclic voltammetry (CV) and differential pulse voltammetry (DPV) measurements were performed with a CHI832B electrochemical analyzer (Shanghai CH Instrument Company, China). Electrochemical impedance spectroscopy (EIS) measurements were carried out on a CHI660C electrochemical workstation (Shanghai CH Instrument Company, China). All electrochemical experiments were performed with a conventional three-electrode system comprising a gold working electrode, a platinum wire auxiliary electrode, and an Ag/AgCl reference electrode. The EIS measurements were performed in a solution of 1 mM $K_4Fe(CN)_6/K_3Fe(CN)_6$ in phosphate-buffered saline (PBS buffer, 25 mM, pH 7.4, 0.1 M KCl). The scanning electron microscopy (SEM) images were obtained on a Hitachi S-4300 scanning electron microscope (Japan).

### 2.3. Preparation of gold nanostructure modified electrode

Prior to use, a bare Au disk electrode was polished sequentially with 1 μm, 0.3 μm, and 0.05 μm alumina slurry and ultrasonicated thoroughly in acetone and water. The well-polished electrode was then subjected to electrochemical pretreatment by cycling the potential between −0.2 and 1.5 V in $H_2SO_4$ (0.5 M) at a scan rate of 100 mV $s^{-1}$ until a stable cyclic voltammogram was obtained, and then the cleaned electrode was allowed to be dried at room temperature. The pH values of 5 mM $HAuCl_4$ were adjusted to a fixed value with NaOH and HCl solution and were aged for about 12 h. Gold nanostructures were electrodeposited on planar gold electrode at a constant potential of 0.5 V at room temperature.

### 2.4. DNA immobilization and hybridization

The probe DNA immobilization on gold nanostructure modified electrode was performed by dropping 20 μL of 0.1 μM probe DNA solution in 25 mM PBS (pH 7.4, 0.1 M KCl) on the electrode surface for 8 h. The DNA-modified electrode was further treated with 1 mM MCH for 30 min to obtain a well aligned DNA monolayer, following by washing with PBS buffer solution and double distilled water to remove unspecific absorbed DNA. For the execution of DNA hybridization, probe DNA immobilized electrode was immersed into stirred 1 mL PBS buffer solution containing different concentration of target DNA for 1.5 h at 37 °C. Then the electrodes were taken out and rinsed with PBS buffer solution and double distilled water and dried with nitrogen.

### 2.5. DNA hybridization detection with an electrochemical indicator of RuHex

The probe DNA or hybridized electrodes were firstly immersed into 50 μM RuHex in 25 mM PBS (pH = 7.4) for 20 min, and then DPV measurements were recorded in blank PBS solution. All the electrochemical measures were carried out under the atmosphere of nitrogen.

## 3. Results and discussion

### 3.1. Electrodeposition of gold nanostructures on the Au substrate

Schematic representation of the fabrication procedure of DNA biosensor is shown in Fig. 1. The gold nanostructure modified electrode was firstly prepared by an electrochemical deposition strategy and then used as the substrate for DNA immobilization and hybridization.

Fig. 2 shows the SEM images obtained for the gold nanostructures electrodeposited at different pHs on gold substrate. It could be seen that, at pH 2.0, the irregular gold nanoparticles with relatively smooth surface were obtained and closely occupied the whole electrode surface at deposition time of 240 s (Fig. 2A). At pH 3.0, the popcorn-like gold nanostructures composed with aggregated nanocrystals were clearly illustrated (Fig. 2B). Under pH 4 condition, the popcorn-like gold nanostructures became more

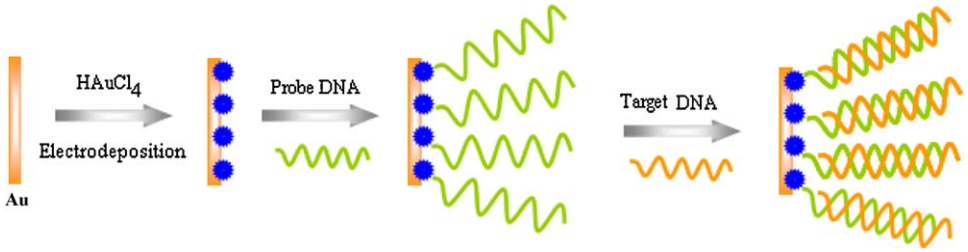


**Fig. 1.** Schematic illustration of the fabrication steps of the electrochemical DNA biosensor.

roundish and rougher and the diameter was increased to be about 220 nm (Fig. 2C). With the further adjustment of pH to 5 and 6, some blossom-bud like particles could be observed on the substrate (Fig. 2D and E). The particle surface was not simply aggregated by the small round gold nanocrystals but appeared with some sheet-like nanoplates.

On prolonging the reaction time from 240 s to 480 s at pH 5.0, the hierarchical nanoflowers up to about 400 nm had been developed, which were built by many nanoplates with the thickness of about 20 nm as building blocks (Fig. 3A). When the deposition time is further prolonged to be 600 s, only protruding nanoplates but no single nanoflower could be observed on the electrode surface (Fig. 3B). This indicates that the nanoflowers have grown into one ensemble with deposition time on the electrode surface. Therefore, the morphology of electrodeposited gold nanostructures could be controlled to some extent by careful adjustment of the pH value of precursor solution and deposition time.

It is well known that the $Cl^-$ from a complex anion of $[AuCl_4]^-$ will be gradually displaced by the $OH^-$ till the final form of $[Au(OH)_4]^-$ with the pH increase (Guo et al., 2007b; Moreau et al., 2005). It is followed by the color change of $HAuCl_4$ solution from yellow to nearly colorless with the pH increase. Also, the color change could be reversed with the decrease of pH again by adding HCl. The hydrolysis process of $[AuCl_4]^-$ could

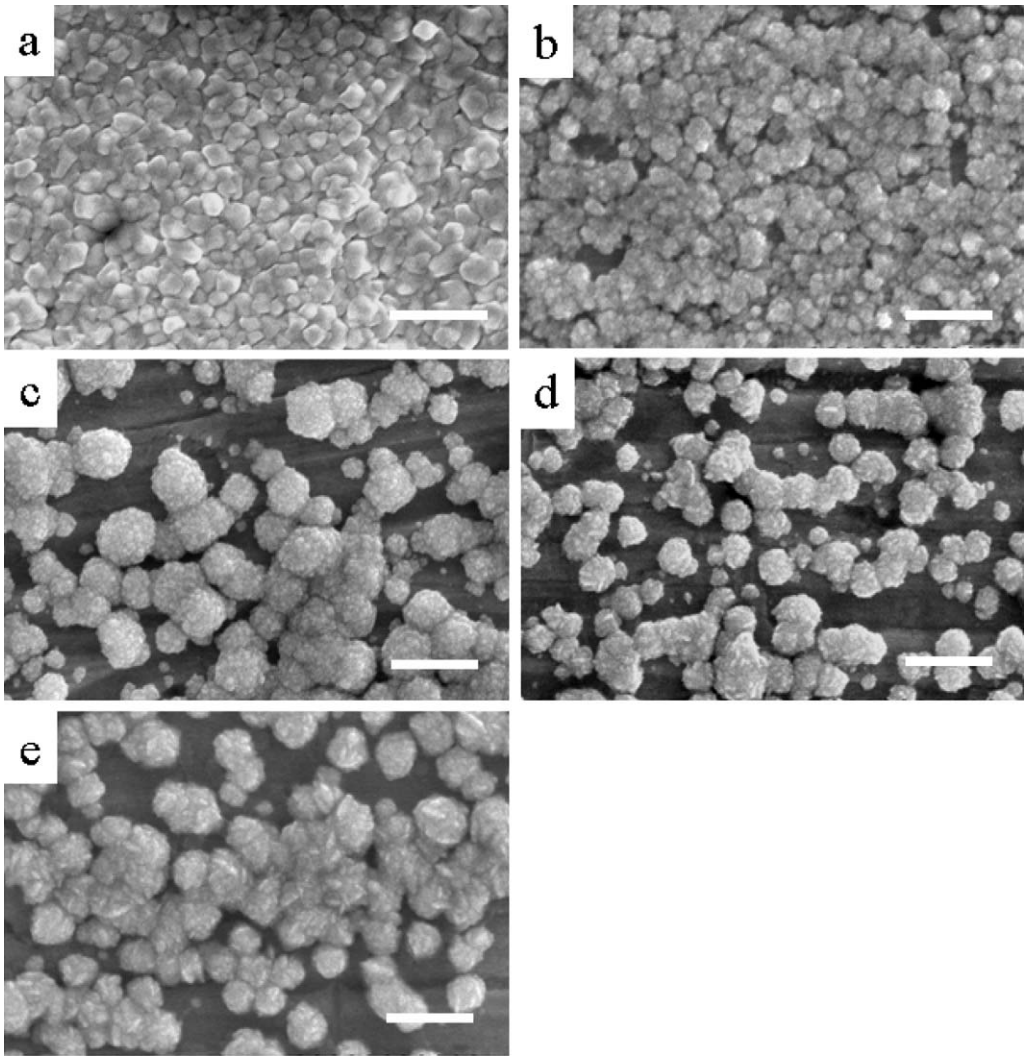


**Fig. 2.** SEM of gold nanostructure modified electrode by a simple electrodepositon method in 5 mM $HAuCl_4$ solution with different pHs (a) 2, (b) 3, (c) 4, (d) 5 and (e) 6. Deposition potential and time is 0.5 V and 240 s, respectively. The scale bar in each case is 500 nm.

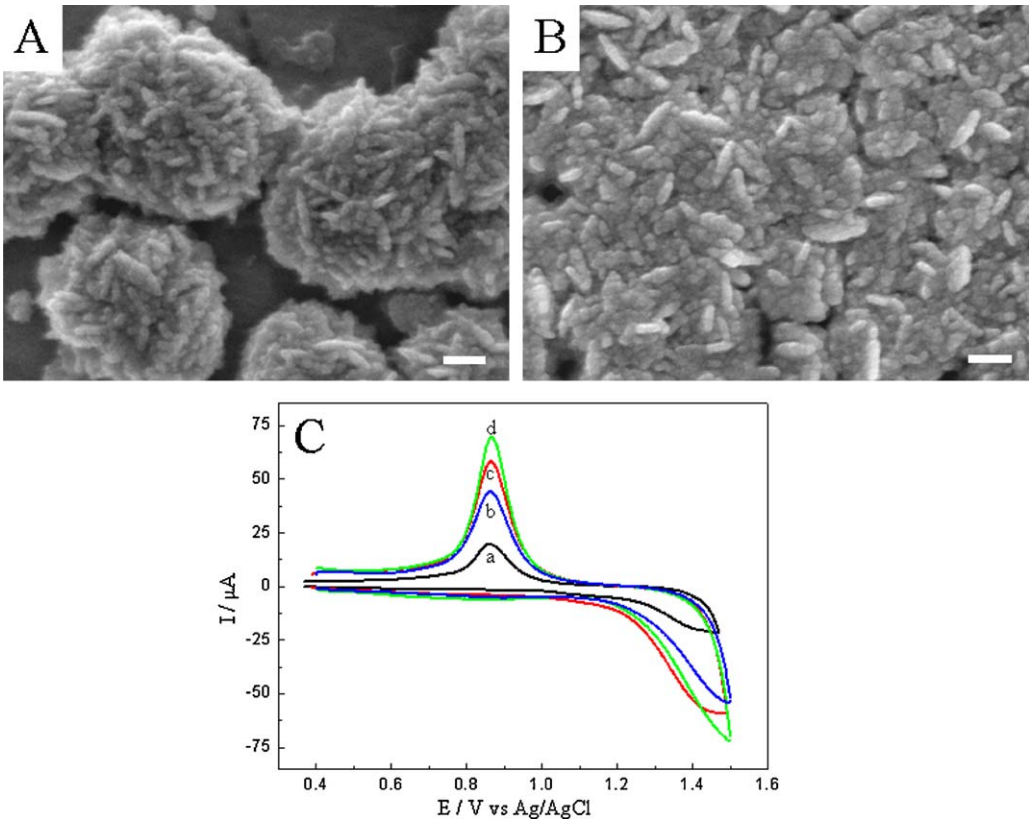


**Fig. 3.** (A) and (B) The high resolution SEM images of gold nanoflowers electrodeposited in 5 mM $HAuCl_4$ with pH 5.0 for 480 s and 600 s, respectively; (C) the cyclic voltammogram in aqueous 0.5 M $H_2SO_4$ solution for the gold nanoflower modified (b–d) and planar (a) gold electrodes. The electrodes of (b), (c) and (d) are obtained by electrodeposition in 5 mM $HAuCl_4$ with pH 5.0 for 240 s, 480 s and 600 s, respectively. Scan rates were all 100 mV $s^{-1}$.

be demonstrated by Eqs. (1)–(4) (Guo et al., 2007b; Zhang et al., 2008a).

$$[AuCl_4]^- + H_2O \leftrightharpoons [AuCl_3(OH)]^- + H^+ + Cl^- \quad (1)$$

$$[AuCl_3(OH)]^- + H_2O \leftrightharpoons [AuCl_2(OH)_2]^- + H^+ + Cl^- \quad (2)$$

$$[AuCl_2(OH)_2]^- + H_2O \leftrightharpoons [AuCl(OH)_3]^- + H^+ + Cl^- \quad (3)$$

$$[AuCl(OH)_3]^- + H_2O \leftrightharpoons [Au(OH)_4]^- + H^+ + Cl^- \quad (4)$$

The different forms of gold complex result in different redox potential and, therefore, lead to the different reduction rate of gold atoms and the morphologies of final gold nanostructures (Lee et al., 2007; Martín et al., 1997). The standard reduction potentials of gold hydroxide complexes are lower than that of $AuCl_4^-$. The typical current–time ($I$–$t$) curves during the electrochemical deposition process are also recorded (see Fig. S1 in the Supplementary Information). It could be seen that the currents decayed in the initial period, and gradually reached a stabilized value, which corresponds to the nucleation and growth process. At lower pH value such as pH 2 and 3, $AuCl_4^-$ is prevalent, which reduces to gold atoms at a comparatively high rate, and thus the current exhibits a transient sharp drop and the stable current values are much higher than others. With the pH increasing, the values of the initial decay and the stabilized currents become smaller, indicating that the reduction rate of gold decreases with the increase of pH because of the generation of gold hydroxide complexes. Higher reduction rate could lead to generation of a larger number of nuclei on the substrate and the final particles are easily agglomerated. Thus, the obtained gold nanoparticles on the electrode surface have a high density and comparably small size. With the pH increase, the reduction rate of gold slows and the initial nuclei on the substrate decreases. The further growth rate of gold onto the nuclei dominates the morphology of gold nanostructures. The growth rate of gold at pH 4 is considered to be comparably faster than that at higher pHs 5 and 6. Thus, the gold nanoparticle with a larger size could be obtained at pH 4.0 and packed more densely by small gold nanocrystals. The relatively slow growth rate at pHs 5 and 6 leads to the loosely packed gold nanocrystals and the flower-like nanostructures with the nanoplates as the building blocks are finally formed. In short, the final morphologies were controlled by the rates of nucleation and growth, which were determined by the pH value of the solutions. Zhang et al. (2008a) have electrochemically synthesized gold nanostructures with different morphology onto glassy carbon substrate by controlling the pH value of precursor solution. Herein, planar gold substrate was employed and the morphology of deposited gold nanostructures was some different from that on glassy carbon substrate. Especially, the gold nanoflowers with the nanoplates as building blocks were interestingly obtained at pH 5.0. The advised planar gold substrate is considered to have an important role in the nucleation rate of gold atoms on the substrate and the further morphology of electrodeposited gold nanostructures. But the detailed role is still not very clear till now.

The cyclic voltammetric curves scanned in 0.5 M $H_2SO_4$ for the gold nanoflower modified and planar gold electrodes are recorded in Fig. 3C. The reductive peak at the potential of about 0.9 V is relative with the reduction of gold oxide formed in the positive potential scan. Its peak area could reflect the relative surface area of gold electrode (Trasatti and Petrii, 1992). Based on the area integration of this cathodic peak, the relative surface area of gold electrode could be evaluated. It could be obtained that the surface area of gold nanoflowers electrodeposited at pH 5.0 is significantly larger than that of planar gold electrode. The surface area of gold nanoflower modified electrodes obtained at pH 5.0 for 240 s, 480 s and 600 s is about 2.7, 3.9, 3.2 times, respectively, of that of planar gold

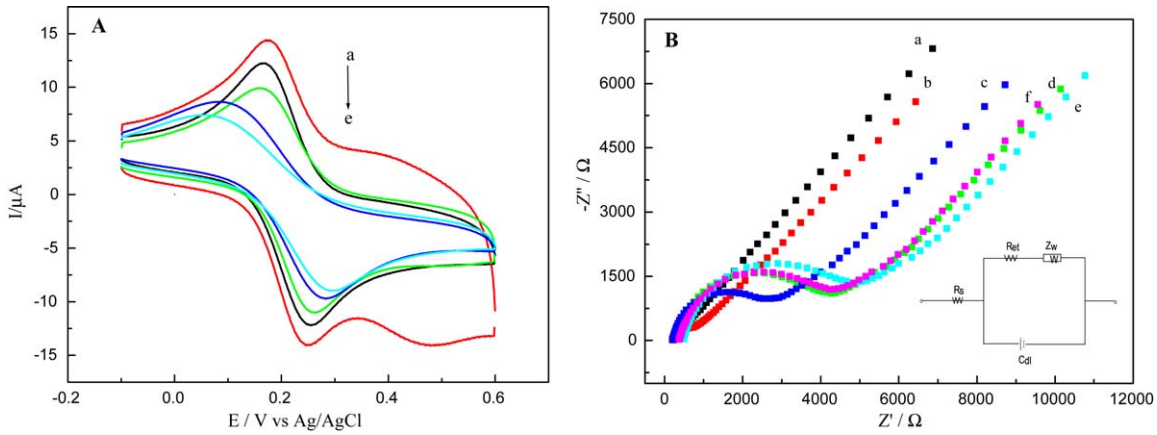


**Fig. 4.** Cyclic voltammograms (A) and electrochemical impedance spectroscopy (B) obtained for bare (b), gold nanoflower modified (a), only thiolated ssDNA immobilized (c), thiolated ssDNA and MCH immobilized (d), hybridized with complementary target DNA (e) and non-complementary target DNA (f) on nanoflower modified electrode in 1 mM $Fe(CN)_6^{3-/4-}$ of 25 mM PBS buffer (pH 7.4, 0.1 M KCl). The scan rate for CV is 100 mV $s^{-1}$ and the frequency for EIS is varied from 0.1 Hz to 10 kHz. The concentrations of complementary and non-complementary target DNA are both 0.1 μM.

electrode. Based on the unique nanostructure and surface area effect, the gold nanoflower modified electrode obtained at pH 5.0 for 480 s is developed for the following DNA biosensor fabrication.

### 3.2. Electrochemical behaviors of $[Fe(CN)_6^{3-/4-}]$ at gold nanoflower modified electrode

The biosensor fabrication process could be monitored based on the electron transfer of ferricyanide through the modified electrode. Fig. 4A shows the cyclic voltammograms obtained for differently modified electrodes in 1 mM $Fe(CN)_6^{3-}/Fe(CN)_6^{4-}$ of 25 mM PBS solution (pH 7.4, 0.1 M KCl) at the scan rate of 100 mV $s^{-1}$. A pair of well-defined redox peaks could be observed at the bare gold electrode with the anodic ($E_{pa}$) and cathodic ($E_{pc}$) peak potential of 0.25 V and 0.17 V, respectively, and a peak to peak potential separation of about 80 mV (curve b). These peaks could be definitely attributed to the redox behaviors of $[Fe(CN)_6^{3-/4-}]$. The electrodeposition of gold nanoflowers induced a larger background current compared with that of bare gold electrode (curve a). Also a pair of broad peaks at about 0.45 V were observed, which could be attributed to the adsorption of $[Fe(CN)_6^{3-/4-}]$ on the gold nanoflower surface. The direct immobilization of probe DNA on modified electrode surface induced a decrease of peak current, indicating that the probe DNA has been successfully immobilized on the electrode surface and the peak current decrease could be well assigned to the repellence of $[Fe(CN)_6^{3-/4-}]$ by the negatively charged phosphate backbone of probe DNA(curve c). The post treatment of MCH induced a continued decrease of peak current and an increase of peak to peak potential separation (curve d). This could be ascribed to the diffusion suppression of $[Fe(CN)_6^{3-/4-}]$ toward the electrode surface by the formed relatively compact assembly monolayer of MCH. When the hybridization of probe DNA immobilized electrode with complementary target DNA was proceeded, the peak current of $[Fe(CN)_6^{3-/4-}]$ was observed with a further decrease. The introduction of complementary DNA increases the negative charge responsible for the increased repellence of redox species (curve e).

EIS could provide further information on the impedance changes of the electrode surface during the modification process. In EIS, the semicircle diameter could represent the electron-transfer resistance, $R_{et}$, which dominate the electron transfer kinetics of the redox probe at the electrode interface. Fig. 4B shows the plots of differently modified electrodes in 1.0 mM $K_3Fe(CN)_6/K_4Fe(CN)_6$ containing 25 mM PBS solution and 0.1 M KCl at open circuit potential with the frequency varied from 0.1 Hz to 10 kHz. The planar gold electrode witnessed a very small $R_{et}$ value of about 460 Ω (curve b). After gold nanoflower modification, an almost straight line was observed, indicating an improvement of electron transfer ability of $[Fe(CN)_6^{3-/4-}]$ by the modified gold nanoflower (curve a). The immobilization of probe DNA monolayer on electrode surface makes an increase of $R_{et}$ to be 2701 Ω (curve c), which could be ascribed to the repellence of redox probe from approaching electrode surface by negative-charged phosphate skeletons of DNA. The following post-treatment with MCH induced an increase of $R_{et}$ to be 4341 Ω (curve d). After hybridization of the immobilized probe DNA with complementary target DNA, the $R_{et}$ was further increased to be 5008 Ω (curve e). Also, it was found that the hybridization with non-complementary target DNA yielded almost no resistance change compared with that of probe DNA and MCH assembled electrode (curve f). The as-observed results fully indicated that the EIS could be used as a feasible tool to monitor DNA hybridization. The impedance experiments for modified electrodes were in good agreement with the results by cyclic voltammetric experiments.

### 3.3. DNA immobilization and hybridization on gold nanoflower modified electrode

The DNA immobilization and hybridization onto different modified electrodes were characterized by differential pulse voltammetry (DPV) experiments with the RuHex as a redox label. DPV was employed herein because it could alleviate the background current effect to a large extent. The DPV results obtained in blank PBS buffer solution after immersion in 50 μM RuHex of 25 mM PBS (pH = 7.4) for 20 min are shown in Fig. 5. The probe DNA modification on the planar gold electrode induced the peak current of about 0.51 μA at the peak potential of about −0.27 V. A peak current increase of about 0.27 μA was observed when the hybridization of probe DNA modified electrode with target DNA. The hybridization efficiency could be obtained based on the calculation of $\Delta I/I_p$. The $\Delta I$ represents the DPV peak current increase of RuHex before and after hybridization with target DNA, and the $I_p$ indicates the DPV peak current of RuHex for the probe DNA immobilized electrode. The hybridization efficiency on the planar gold electrode was obtained as about 53%. The peak current for the probe DNA immobilized onto gold nanoflower modified electrode was about 1.46 μA. The peak current increase after DNA hybridization was about 1.04 μA, indicating a hybridization efficiency of about 69%. It could be obtained that the immobilization amount of probe DNA on gold nanoflowers is not simply proportional with the surface area increase. The

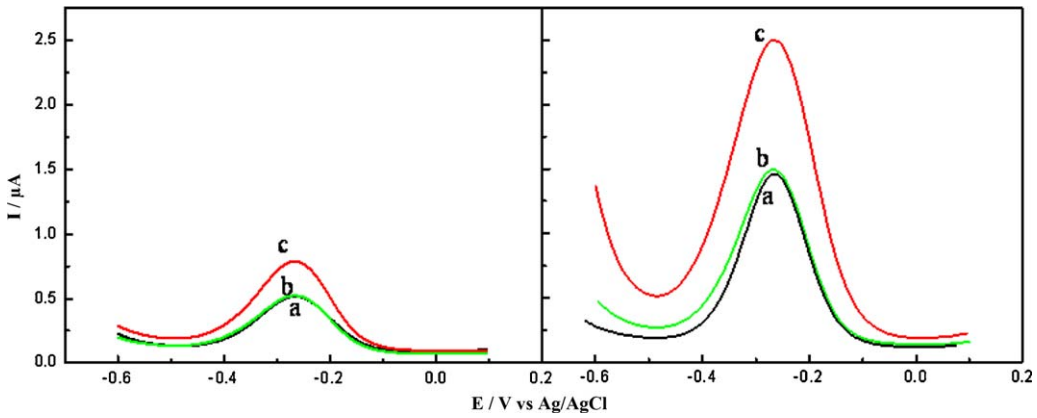


**Fig. 5.** Differential pulse voltammograms of thiolated ssDNA immobilized (curve a), hybridized with non-complementary target DNA (curve b), and complementary target DNA (curve c) onto planar (left) and gold nanoflowers (right) modified electrodes in blank PBS buffer solution after immersion in 50 μM RuHex for 20 min at a scan rate of 100 mV $s^{-1}$.

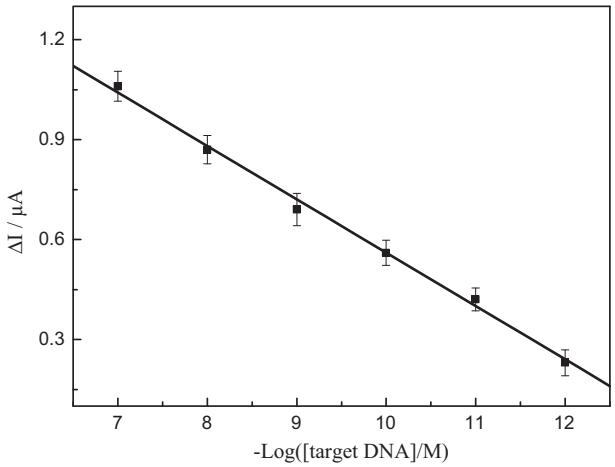


**Fig. 6.** Relation of the DPV peak current increase ($\Delta I$) of RuHex onto gold nanoflower modified electrode before and after DNA hybridization with the logarithm of target DNA concentration from $1 \times 10^{-7}$ M to $1 \times 10^{-12}$ M.

monolayer of probe DNA formed onto gold nanoflowers surface is considered to be more loosely than that on planar gold surface owing to the relatively rough surface of gold nanoflowers. But the hybridization efficiency is largely improved on the gold nanoflower modified electrode. The control experiments performed with the hybridization of probe DNA with non-complementary target DNA on either planar or gold nanoflower modified electrodes demonstrated almost the same responses with that of probe DNA modified electrode (curve b), indicating a good selectivity of current electrochemical DNA biosensor.

### 3.4. Detection limit for target DNA on gold nanoflower modified electrode

The electrochemical hybridization assay was further investigated by varying the target DNA concentration with the use of RuHex as an indicator. The relation of DPV peak current increase ($\Delta I$) of RuHex with decrease in the concentration of target DNA on gold nanoflower modified electrode is displayed in Fig. 6. A linear correlation of peak current increase ($\Delta I$) to the logarithm of the target DNA concentration ranged from 1 pM to 0.1 μM was obtained with a linear regression coefficient of 0.998. Three independent electrodes were used simultaneously for the acquisition of each point in the calibration curve. The low detection limit toward target DNA was obtained as 1 pM onto the gold nanoflower modified electrode. It is comparable with or even higher than that of some reported works based on gold related nanomaterial modification (see Table S1 in the Supplementary Information). Even though some works have reported more high sensitivity, the current direct electrodeposition method for the preparation of gold nanoflowers is more simple and easier to extend for applications in various biosensors fabrication. The detection limit for target DNA on the planar gold electrode has also been obtained as 1 nM (see Fig. S2 in the Supplementary Information). The sensitivity could be upgraded with three orders of magnitude by the use of gold nanoflowers modification.

### 3.5. Regeneration and stability of the fabricated DNA sensor

The regeneration of DNA biosensor is extremely important to practical applications such as clinical diagnoses and biological monitoring. It was found that the fabricated DNA biosensor could be regenerated 8 times with about 15% loss of the original signal by dipping the electrode in hot water (80 °C) for 10 min, followed by a rapid cooling in an ice bath for 10 min. The signal attenuation seemed to be attributed to the loss of thiolated probes on the electrode surface. The regeneration of current DNA biosensor has been compared with some reported works (see Table S2 in the Supplementary Information). At the same time, the stability of the fabricated DNA biosensor was investigated. The probe DNA modified electrode was firstly stored in the refrigerator at 4 °C over 2 weeks and then examined by DPV after its hybridization with complementary target DNA. Experiments demonstrated that the DNA biosensor retained about 86% of its initial response.

## 4. Conclusions

A simple one-step electrodeposition method was used to fabricate gold nanostructure modified electrodes. The morphology of modified electrode could be controlled to some extent by changing the pH value of precursor solution and deposition time. The gold nanoflowers with the nanoplates as the building blocks could be obtained at pH 5.0. With the use of RuHex as a redox indicator, the fabricated electrochemical DNA biosensor based on gold nanoflower modified electrode could achieve a low detection limit of 1 pM toward the detection of target DNA, which is about there orders of magnitude larger than that on the planar gold electrode. Furthermore, this electrode modification strategy is also expected for extensive applications in protein, enzyme biosensors.

## Acknowledgements

This research was supported by the National Natural Science Foundation of China (No. 21005043, No. 20775039), the Natural Science Foundation of Shandong Province of China (Nos. Q2008B05, ZR2009BM031, ZR2009BM013, 2009ZRB01393), and open project of Beijing National Laboratory for Molecular Sciences.

## Appendix A. Supplementary data

Supplementary data associated with this article can be found, in the online version, at doi:10.1016/j.bios.2011.09.003.

## References

Chang, H., Yuan, Y., Shi, N., Guan, Y., 2007. Anal. Chem. 79, 5111–5115.
Chen, C., Ganguly, A., Wang, C., Hsu, C., Chattopadhyay, S., Hsu, Y., Chang, Y., Chen, K., Chen, L., 2009. Anal. Chem. 81, 36–42.
Drummond, T.G., Hill, M.G., Barton, J.K., 2003. Nat. Biotechnol. 21, 1192–1199.
Duan, X., Li, Z., He, F., Wang, S., 2007. J. Am. Chem. Soc. 129, 4154–4155.
Gunnarsson, A., Jönsson, P., Marie, R., Tegenfeldt, J.O., Höök, F., 2008. Nano Lett. 8, 183–188.
Guo, S., Wang, L., Wang, E., 2007a. Chem. Commun., 3163–3165.
Guo, Z., Zhang, Y., Huang, L., Wang, M., Wang, J., Sun, J., Xu, L., Gu, N., 2007b. J. Colloid Interface Sci. 309, 518–523.
Hu, K., Lan, D., Li, X., Zhang, S., 2008. Anal. Chem. 80, 9124–9130.
Katz, E., Willner, I., Wang, J., 2004. Electroanalysis 16, 19–44.
Kannan, B., Williams, D.E., Booth, M.A., Travas-Sejdic, J., 2011. Anal. Chem. 83, 3415–3421.
Kim, D., Kerman, K., Saito, M., Sathuluri, R.R., Endo, T., Yamamura, S., Kwon, Y., Tamiya, E., 2007. Anal. Chem. 79, 1855–1864.
Lee, J.H., Kamada, K., Enomoto, N., Hojo, J., 2007. J. Colloid Interface Sci. 316, 887–892.
Li, F., Han, X., Liu, S., 2011. Biosens. Bioelectron. 26, 2619–2625.
Li, Z.-P., Liu, C.-H., Fan, Y.-S., Duan, X.-R., 2007. Anal. Bioanal. Chem. 387, 613–618.
Li, H., Sun, Z., Zhong, W., Hao, N., Xu, D., Chen, H.-Y., 2010. Anal. Chem. 82, 5477–5483.
Liu, G., Wan, Y., Gau, V., Zhang, J., Wang, L., Song, S., Fan, C., 2008. J. Am. Chem. Soc. 130, 6820–6825.
Liu, S., Liu, J., Han, X., Cui, Y., Wang, W., 2010. Biosens. Bioelectron. 25, 1640–1645.
Martín, H., Carro, P., Hernández Creus, A., González, S., Salvarezza, R.C., Arvia, A.J., 1997. Langmuir 13, 100–110.
Minunni, M., Tombelli, S., Fonti, J., Spiriti, M.M., Mascini, M., Bogani, P., Buiatti, M., 2005. J. Am. Chem. Soc. 127, 7966–7967.
Moreau, F., Bond, G.C., Taylor, A.O., 2005. J. Catal. 231, 105–114.
Munde, M., Ismail, M.A., Arafa, R., Peixoto, P., Collar, C.J., Liu, Y., Hu, L., David-Cordonnier, M., Lansiaux, A., Bailly, C., Boykin, D.W., Wilson, W.D., 2007. J. Am. Chem. Soc. 129, 13732–13743.
Patolsky, F., Lichtenstein, A., Willner, I., 2000. J. Am. Chem. Soc. 122, 418–419.
Qiu, L.-P., Wu, Z.-S., Shen, G.-L., Yu, R.-Q., 2011. Anal. Chem. 83, 3050–3057.
Sassolas, A., Leca-Bouvier, B.D., Blum, L.J., 2008. Chem. Rev. 108, 109–139.
Seefeld, T.H., Zhou, W.-J., Corn, R.M., 2011. Langmuir 27, 6534–6540.
Seo, B., Choi, S., Kim, J., 2011. ACS Appl. Mater. Interface 3, 441–446.
Soleymani, L., Fang, Z., Sun, X., Yang, H., Taft, B.J., Sargent, E.H., Kelley, S.O., 2009. Angew. Chem. Int. Ed. 48, 8457–8460.
Steel, A.B., Herne, T.M., Tarlov, M.J., 1998. Anal. Chem. 70, 4670–4677.
Taton, T.A., Mirkin, C.A., Letsinger, R.L., 2000. Science 289, 1757–1760.
Trasatti, S., Petrii, O.A., 1992. J. Electroanal. Chem. 327, 353–376.
Wang, J., 2003. Anal. Chim. Acta 500, 247–257.
Weizmann, Y., Patolsky, F., Katz, E., Willner, I., 2003. J. Am. Chem. Soc. 125, 3452–3454.
Yang, R., Jin, J., Chen, Y., Shao, N., Kang, H., Xiao, Z., Tang, Z., Wu, Y., Zhu, Z., Tan, W., 2008. J. Am. Chem. Soc. 130, 8351–8358.
Zhang, H., Xu, J., Chen, H., 2008a. J. Phys. Chem. C 112, 13886–13892.
Zhang, J., Qi, H., Li, Y., Yang, J., Gao, Q., Zhang, C., 2008b. Anal. Chem. 80, 2888–2894.
Zhang, S., Wu, Z., Shen, G., Yu, R., 2009. Biosens. Bioelectron. 24, 3201–3207.
Zhu, D., Tang, Y., Xing, D., Chen, W.R., 2008. Anal. Chem. 80, 3566–3571.
Zhu, C., Meng, G., Huang, Q., Huang, Z., Chu, Z., 2011. Cryst. Growth Des. 11, 748–752.